Journal of Sound and Vibration (1998) **210**(3), 351–365

FLEXURAL–TORSIONAL COUPLING EFFECT ON VIBRATIONAL CHARACTERISTICS OF ANGLE-PLY LAMINATES

T. Maeda, V. Baburaj, Y. Ito and T. Koga

Institute of Engineering Mechanics, University of Tsukuba, Tsukuba Science City, Japan

(*Received* 17 *March* 1997, *and in final form* 18 *September* 1997)

A mainly experimental investigation is presented on the vibrational characteristics of angle-ply laminate made of carbon/epoxy composite material, considering the effect of flexural–torsional coupling stiffness. This consists of a resonance test on a cantilevered laminated plate model by using laser holographic interferometry. An exact comparison of the coupling effect was achieved by employing two special types of angle-ply laminates, each consisting of eight plies in which one type had the least possible, and the other type, no coupling stiffness at all. The observed results show that the effect of flexural–torsional coupling stiffness on the resonance frequencies is only marginal. By contrast, the vibrational mode shapes are found to be affected considerably by the coupling stiffness. Moreover, the amount of this coupling effect is also observed to depend both on the fiber orientation and the aspect ratio of the plate model. An analytical study was also conducted by using the Ritz energy method and a good agreement between the experimental and the theoretical values is observed upon comparison.

1. INTRODUCTION

Symmetrically fabricated angle-ply laminates, in general, have the flexural–torsional coupling stiffnesses expressed as D_{16} and D_{26} in the constitutive relation between moment resultants and curvatures. In the application of those laminated plates as the components of a structural system, the presence of these coupling stiffnesses may yield undesirable mechanical behaviors. For a symmetric angle-ply laminate, these coupling stiffness values decrease as the number of laminae increases and hence the laminate thickness. Therefore, to take advantage of angle-ply laminates in thin aerospace structures, the laminate is very often a symmetric one with flexural–torsional coupling stiffness. Dynamic studies of cantilevered anisotropic laminates having D_{16} and D_{26} coupling stiffness have been carried out by several authors [1–3]. Jensen and Crawley [4] mainly conducted theoretical estimations of frequencies and mode shapes by comparing the three types of solution techniques, namely, partial Ritz, Rayleigh–Ritz and finite element methods, and concluded that chordwise flexure had to be considered in any analysis of bending–torsion coupling. The Ritz method with algebraic polynomial displacement function has been employed by Narita and Leissa [2], and is shown to give accurate upper bounds of frequencies. For various boundary conditions of more complicated plate vibrational problems, the polynomial functions have also been employed by Laura *et al*. [5, 6] for isotropic material, and by Qatu for composite material [7]. Effects of sweep angle on frequencies and associated mode shape have been examined by Fukunaga *et al*. [8] for a composite wing model using lamination parameters. In these studies, although the effect of the coupling stiffness on the mode shapes can be identified theoretically, no experimental result is

0022–460X/98/080351 + 15 $25.00/0/sv971331

available. For the unidirectional filamentary composite material panels suspended by strings, the experimentally measured nodal patterns obtained with a hand-held velocity probe have been presented by Clary [9]. However, the coupling effect both on frequency and mode shape with the model behavior of laminates has not received much research attention and has not so far been addressed especially by experiment to the best of our knowledge.

An attempt has therefore been made in this paper to understand the influence of the flexural–torsional coupling stiffness on the vibrational characteristics of angle-ply laminates using experimental methods. The experimental results obtained by holographic interferometry have also been compared with analytical results employing the Ritz method. It has been proven theoretically that the flexural–torsional coupling stiffness vanishes to zero in some cases of angle-ply laminates [10]. This requires a special stacking sequence of the laminate, namely, a symmetric–antisymmetric configuration about the middle surface of the plate symbolically expressed as

$$[(A)/(-A)], \tag{1}$$

where

$$(A) = (+\theta/-\theta/-\theta/+\theta) \qquad \text{and} \qquad (-A) = (-\theta/+\theta/+\theta/-\theta). \tag{2}$$

The bending stiffness matrix of a laminate defined by equation (1) can be written as

$$D_{ij} = \begin{bmatrix} D_{11} & D_{12} & 0 \\ D_{12} & D_{22} & 0 \\ 0 & 0 & D_{66} \end{bmatrix} \qquad i, j = 1, 2, 6. \tag{3}$$

It must consist of a minimum of eight plies of equal thickness, each for a chosen fiber orientation. Although this laminate is not symmetric with respect to its mid-plane, the coupling matrix that gives coupling between extension and bending also vanishes completely.

On the other hand, if we fabricate a symmetric laminate which has a composition of

$$[(A)/(A)], \tag{4}$$

its stiffness matrix becomes

$$D_{ij} = \begin{bmatrix} D_{11} & D_{12} & D_{16} \\ D_{12} & D_{22} & D_{26} \\ D_{16} & D_{26} & D_{66} \end{bmatrix} \qquad i, j = 1, 2, 6. \tag{5}$$

The values of D_{16} and D_{26} remain, whereas all the other stiffnesses including the extensional stiffness matrix are equal to the values of a special symmetric–antisymmetric angle-ply laminate denoted by equation (1). For the symmetric laminate, though the magnitude of the coupling stiffness can be varied by varying the stacking sequence, the stacking of an eight-ply laminate considered here has the minimum values of coupling stiffness possible. In other words, the two different laminates whose stackings are defined by equations (1) and (4) exhibit identical elastic properties except for the presence of flexural–torsional coupling stiffness. Moreover, the resulting coupling stiffness of the symmetric laminate considered have minimum possible values among the eight-ply laminate. Therefore, by comparing the vibrational characteristics of the above mentioned two types of laminates, the influence of the flexural–torsional coupling stiffness could be studied exactly. In the experiment, a laser holographic interferometry was used to measure the resonance

frequencies and to record the mode shapes of a cantilevered laminate, whereas the analytical study was carried out using the Ritz method.

2. EXPERIMENTAL PROCEDURE

In the experiment, laser holographic interferometry was employed to investigate the vibrational characteristics of the angle-ply laminates. In general, the undeformed image of a test specimen must be recorded first, especially in the real-time method. This procedure can be achieved without difficulty by using a thermoplastic plate as the film plate. The thermoplastic plate consists of a clear conductive coating layer, a photoconducter layer and a thermoplastic layer, and the principle of recording the hologram is based on a phenomenon in which a heated thermoplastic is deformed by the electrostatic force according to the exposed light intensity. Its characteristics are: development can be done electrically in a few seconds without changing the plate's position; because of high diffraction efficiency, the reconstructed image is bright; and the plate is re-usable. Moreover, by the time-average method using the dry plate, which is more sensitive than the thermoplastic plate, the micro-ordered out-of-plane deflection can be recorded clearly over the whole plate.

Carbon/epoxy laminated plates having seven different fiber orientations, as listed in Table 1, were fabricated, and test specimens were made out of this with a width of $30 \pm 0{\cdot}1$ mm and a thickness of 2·09 mm. Additionally, to understand the effect of clamped boundary, angle-ply laminates having a width of $60 \pm 0{\cdot}1$ mm were also made and tested. The four independent engineering constants of orthotropic fiber composite material were obtained by tensile tests using 0 and 90° laminates [11], and $\pm 45°$ laminate [12]. Measured values of these lamina constants were $E_L = 1{\cdot}02 \times 10^{11}$ N/m^2, $E_T = 7{\cdot}52 \times 10^9$ N/m^2, $v_{LT} = 0{\cdot}328$ and $G_{LT} = 3{\cdot}62 \times 10^9$ N/m^2, which were used to calculate the analytical results. The experimental set-up is shown schematically in Figure 1, in which a 300-mW argon ion laser having a wavelength of 514·5 nm and the associated optical components are placed on a pneumatically supported steel table eliminating any undesired oscillations. Test specimens were very lightly sprayed white over the effective length to achieve higher optical reflectivity.

In the experiment, the specimen was clamped at one end to form a cantilevered plate, and was acoustically excited. Owing to the real-time holographic interferometry, the change of the fringe pattern could be observed through a monitoring system as the excitation frequency swept slowly upwards. When a rapid increase in the fringe number was observed, a peak of the fringe number was determined by fine tuning. Thus, the excitation frequency at that peak was regarded as the resonance frequency of the test specimen. Then, after checking the resonance frequencies by the real-time method, each resonant mode shape was recorded by the time-average method. The holographic plates used here were Agfa 8E56 dry plates, and exposure time was 1 s.

TABLE 1

Test specimens

Material	Composition	Fiber angle (deg.)
Unidirectional	θ_8	0, 90
Symmetric	$(+\theta/-\theta/-\theta/+\theta)$ sym.	15, 30, 45, 60, 75
Anti-symmetric	$(+\theta/-\theta/-\theta/+\theta)$ anti-sym.	15, 30, 45, 60, 75

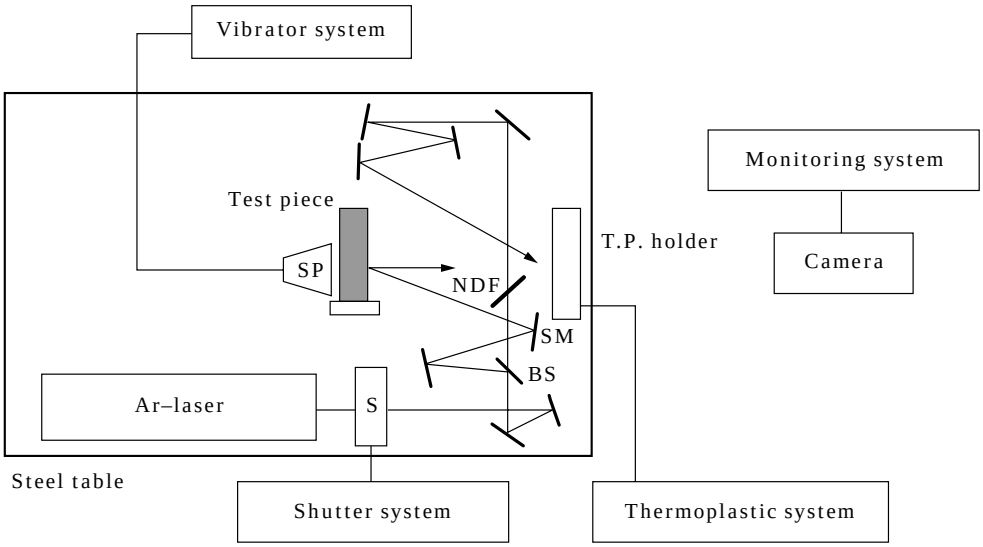

Figure 1. Schematic apparatus of laser holography. NDF: ND filter; SM: spherical mirror; BS: beam splitter; S: shutter; SP: speaker; /: mirror.

3. RITZ METHOD

The Ritz method has been employed to calculate the resonance frequencies and the mode shapes. For a cantilevered laminated plate having length, width, and thickness defined by a, b and h, respectively (see Figure 2), the maximum strain energy, V_{max}, and the maximum kinetic energy, T_{max}, can be written in the non-dimensional forms of

$$V_{max} = \tfrac{1}{2}(D_0/\alpha a^2)\int_0^1\int_{-1}^1 \{\kappa^*\}^T[D^*]\{\kappa^*\}\,\mathrm{d}\xi\,\mathrm{d}\eta, \tag{6}$$

$$T_{max} = \tfrac{1}{2}(D_0/\alpha a^2)\Omega^2\int_1^0\int_{-1}^1 W^2\,\mathrm{d}\xi\,\mathrm{d}\eta, \tag{7}$$

where D_0 is taken as a reference bending stiffness and is equal to D_{11} of 90° laminate, and W is the out-of-plane deflection of the plate. The non-dimensional quantities are defined by

$$\xi = x/a, \qquad \eta = y(b/2), \qquad \alpha = a/b, \tag{8}$$

$$\Omega = \omega a^2\sqrt{\rho/D_0}, \qquad [D^*] = [D]/[D_0], \qquad \{\kappa^*\} = \{\partial^2 W/\partial\xi^2 \quad \partial^2 W/\partial\eta^2 2 \quad \partial^2/\partial\xi\,\partial\eta\}^T, \tag{9}$$

where Ω is a frequency parameter, ρ is the mass density per unit area and $[D]$ is the bending stiffness matrix of angle-ply laminate. Narita and Leissa [2] employed a general polynomial series for steady state solution given by the following equation incorporating the plate boundary conditions.

$$W(\xi,\eta) = \sum_{m=2}^{M}\sum_{n=0}^{N} C_{mn}\,\xi^m\eta^n, \tag{10}$$

where C_{mn} are unknown coefficients. Based on the Ritz method, after substituting equation (10) into equations (6) and (7), the total potential energy is minimized by equating the partial derivative of the total potential with respect to each C_{mn} to zero as shown below.

$$\partial(T_{max} - V_{max})/\partial C_{mn} = 0 \ (m = 2, 3, \ldots, M; n = 0, 1, \ldots, N). \tag{11}$$

The above equation yields the eigenvalue formulation expressed as

$$([K] - \Omega^2[L])\{C_{mn}\} = 0, \tag{12}$$

where $[K]$ and $[L]$ are the stiffness and mass coefficient matrices, respectively. By setting the determinant of the resultant coefficient matrix, $(|[K] - \Omega^2[L]|)$, equal to zero, the non-dimensional frequency parameters can be obtained. Then, the coefficients C_{mn} can subsequently be determined using the non-dimensional frequency parameter. The vibrational mode shapes can also be obtained by substituting the determined values of C_{mn} back into equation (10).

In the present study, the theoretical values were calculated by a polynomial series approximation for the deflection shown in equation (10). As a result of the convergence study, it was found that the maximum difference between the predicted frequencies with $(M, N) = (8, 6)$ and $(M, N) = (9, 7)$ was less than 1% for all the cases considered. Therefore, all the theoretical values were calculated by using $(M, N) = (9, 7)$.

4. RESULTS AND DISCUSSION

The measured and calculated values of resonance frequencies for the first six modes of 120×30 mm laminates and the first three modes of 120×60 mm laminates are shown in Figures 3 and 4, respectively. Although the number of the experimental values of frequencies presented in Figure 3 was expected to total 72 cases, tuning of resonance frequencies was not possible for three cases. This was due to limitations of acoustic excitations to higher frequencies and closely spaced frequencies of different modes. In both figures, the differences of the measured frequencies between the two types of the laminates are found to be insignificant and to be similar to those of the analytical predictions by the Ritz method. Therefore, it is concluded that the coupling effect on the resonance frequencies of the symmetric laminates considered in the present study is almost negligible

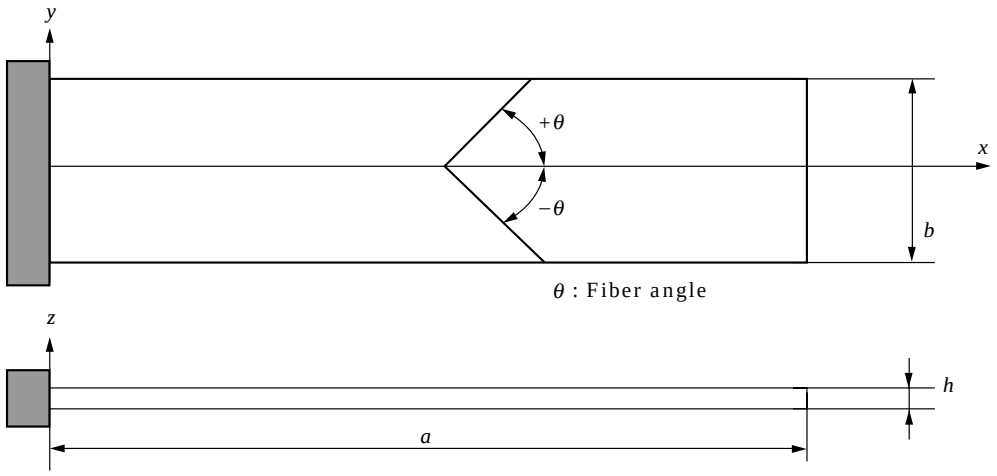

Figure 2. Configuration of test specimen.

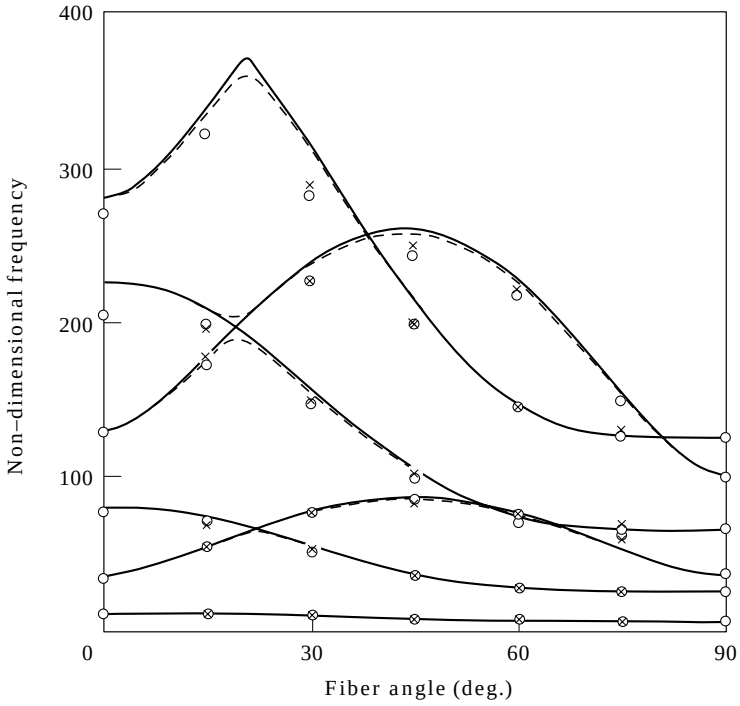

Figure 3. Comparison of non-dimensional frequencies for the first six modes (120 × 30 mm laminates). Ritz: —, anti-symmetric; -----, symmetric. Experimental: ×, anti-symmetric; ○, symmetric.

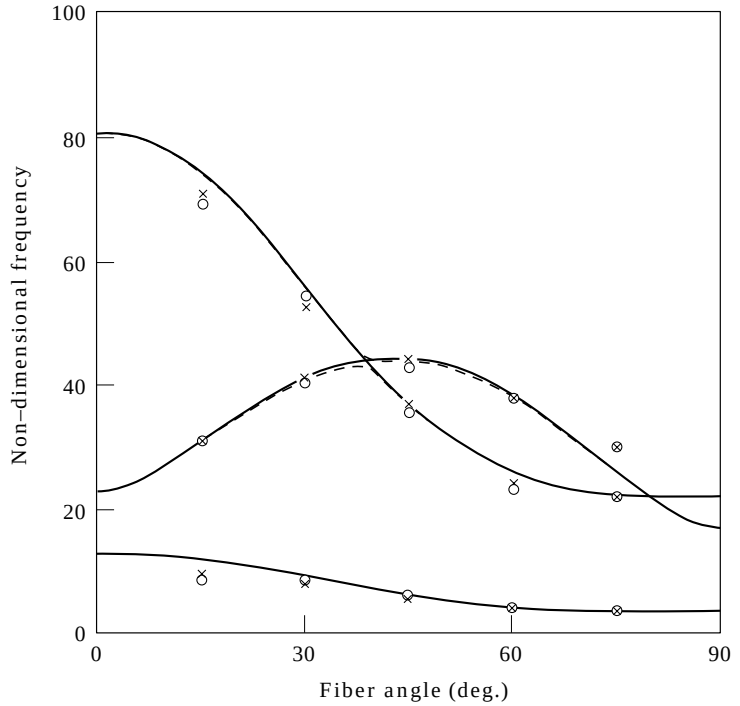

Figure 4. Comparison of non-dimensional frequencies for the first three modes (120 × 60 mm laminates). Ritz: —, anti-symmetric; ----, symmetric. Experimental: ×, anti-symmetric; ○, symmetric.

except at certain particular values of laminate orientation. As seen from Figures 3 and 4, at these particular laminate orientations, the curves for different modes of vibration intersect each other for the case of the anti-symmetric laminate. By contrast, the curves veer away slightly from each other for the symmetric laminate owing to the coupling effect.

In the present experiment, the fringe patterns of the vibrational modes corresponding to the measured resonance frequencies were recorded for all the cases by laser holography. In order to demonstrate the apparent difference between the fringe patterns of the special anti-symmetric and the symmetric laminates, the fringe patterns of some of the selected cases of angle-ply laminates are shown here. Figures 5 and 6 show the fringe patterns for the first six modes of the 15 and 30° laminates, respectively. The photograph for the sixth mode of the special anti-symmetric laminate is not available for the reason mentioned above. Because the fringe patterns are almost symmetrical against the middle chord line of the plate for the special anti-symmetric laminates shown in Figures 5(a) and 6(a), the effect of flexural–torsional coupling being found to be absent is a fact also evidenced by

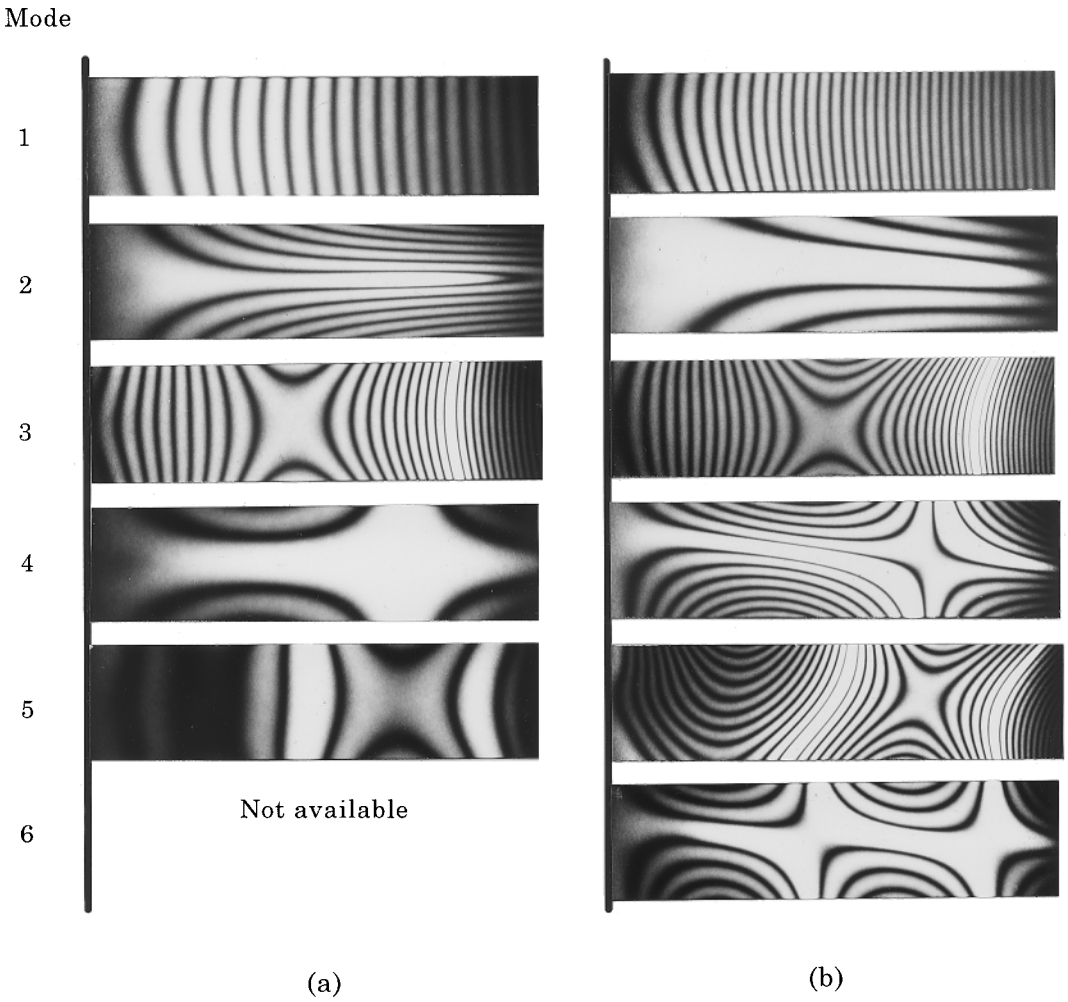

Figure 5. Fringe patterns of the first six modes ($\theta = 15°$, 120 × 30 mm laminates). (a) Anti-symmetric; (b) symmetric.

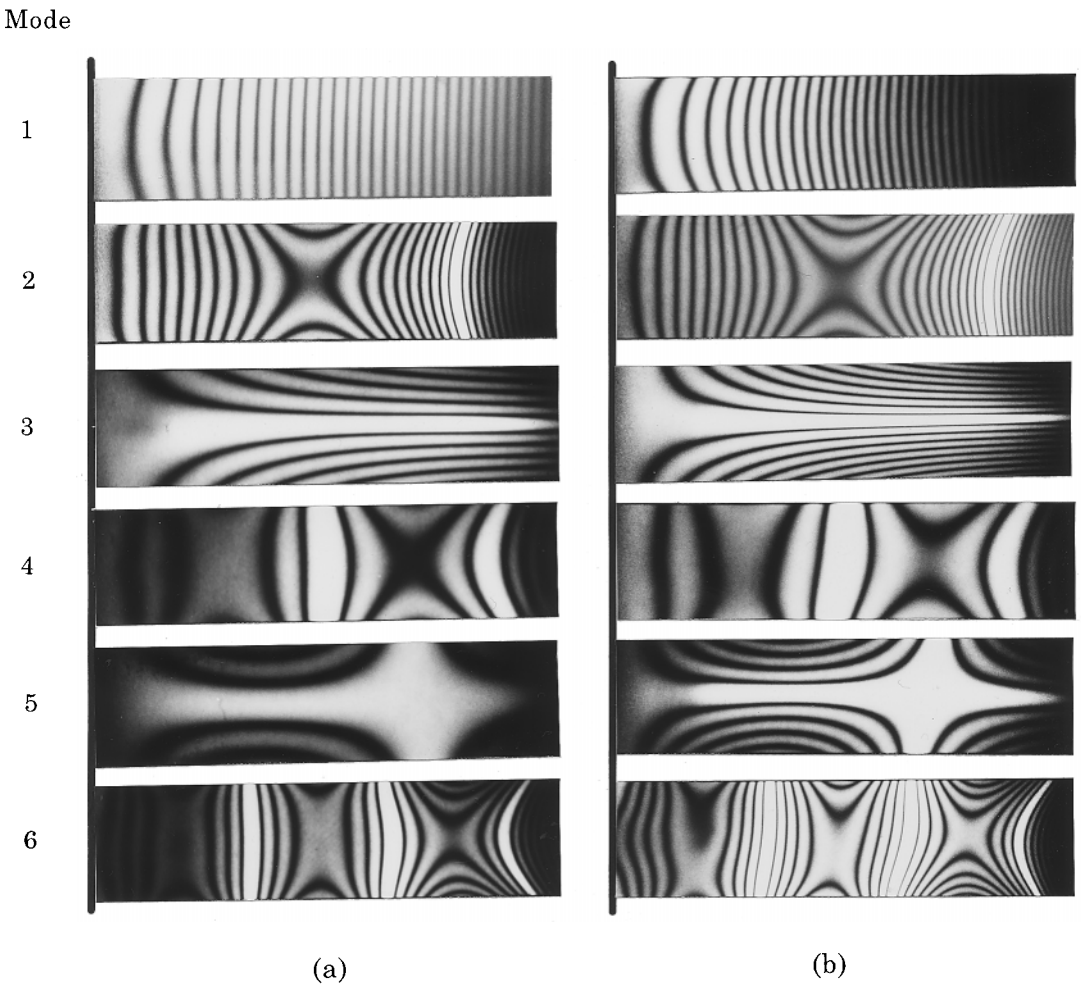

Figure 6. Fringe patterns of the first six modes ($\theta = 30^\circ$, 120×30 mm laminates). (a) Anti-symmetric; (b) symmetric.

the classical lamination theory. On the other hand, for the symmetric laminates shown in Figures 5(b) and 6(b), the fringe patterns are found not to be symmetric against the middle chord line of the plate, indicating that these mode shapes are affected by the flexural–torsional coupling stiffness. Comparison of the same effect for the remaining cases of angle-ply laminates indicates that there is an influence of coupling effect on the obtained mode shapes; however, for the plate aspect ratio of the four cases considered, the coupling effect is found to be decreasing gradually as the fiber orientation increases from 45°. Additionally, the magnitude of this coupling effect could be identified from the fringe patterns of Figures 5 and 6 based on the slope between the chordwise direction and the vertical nodal lines of the flexural vibrations, especially for the second flexural mode. In the next exercise, the second flexural mode is therefore examined more closely for all the cases of fiber orientations and two cases of aspect ratio. For the special anti-symmetric laminates presented in both Figures 7(a) and 8(a), it can also be verified that those laminates have no flexural–torsional coupling stiffness because of the symmetrical fringe

patterns obtained. On the other hand, we can see this coupling effect on the mode shapes for the symmetric angle-ply laminates shown in Figures 7(b) and 8(b). Since the slope of the nodal line corresponding to the second flexural mode is found to be varying with regard to the fiber angle, it is evident that the magnitude of the flexural–torsional coupling effect on the mode shapes depends on the fiber orientation. Moreover, when the width of the plate increases, the clamped boundary effect appears as shown in Figure 8, especially for the 15° laminates. Also, the fringe patterns for the 45, 60 and 75° laminates of Figure 8(b) are found to be unsymmetrical when compared to those of Figure 7(b). This suggests that the degree of the coupling effect depends also on the plate aspect ratio.

In order to establish the above mentioned fact, the relationship of the slope of the second flexural mode's nodal line with respect to the aspect ratio has been studied both analytically and experimentally considering the 15, 30 and 45° symmetric laminates.

These variations, namely, the slope of the nodal line against the plate aspect ratio, are shown in Figure 9. It can be seen from this figure that the slope of the nodal line changes extensively with respect to both plate aspect ratio and fiber orientation, an observation also noted from the results of Figures 7 and 8. The agreement between the results obtained

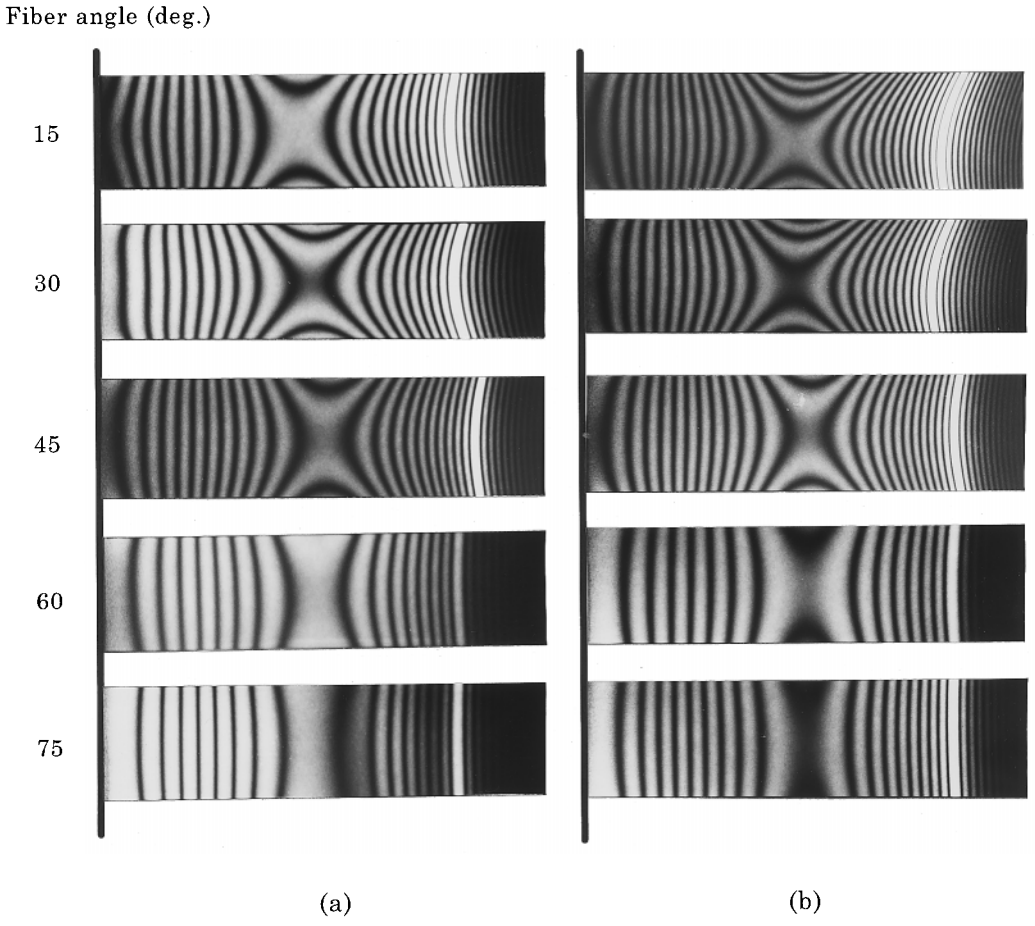

Figure 7. Fringe patterns of the second flexural mode (120 × 30 mm laminates). (a) Anti-symmetric; (b) symmetric.

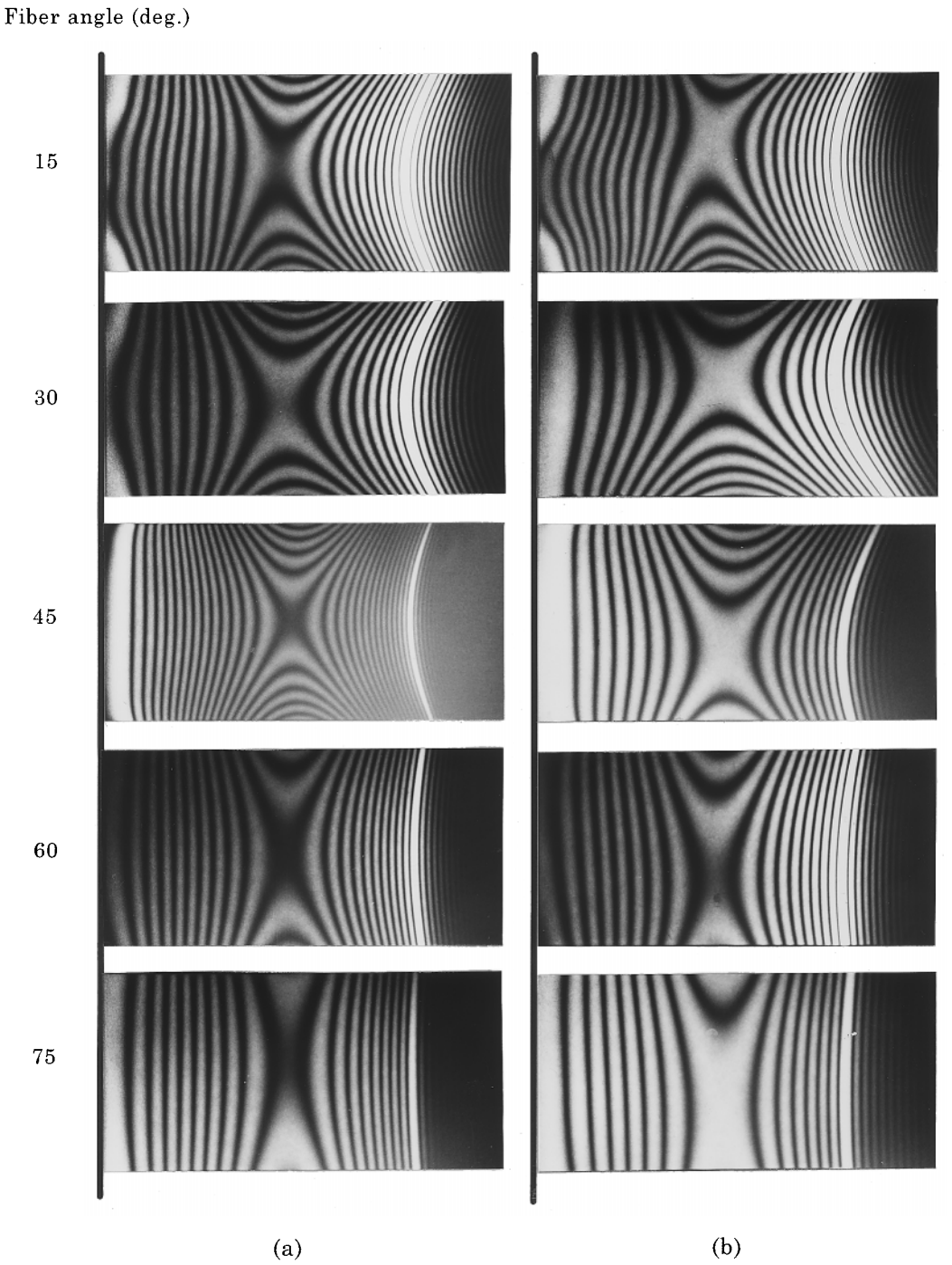

Figure 8. Fringe patterns of the second flexural mode (120 × 60 mm laminates). (a) Anti-symmetric; (b) symmetric.

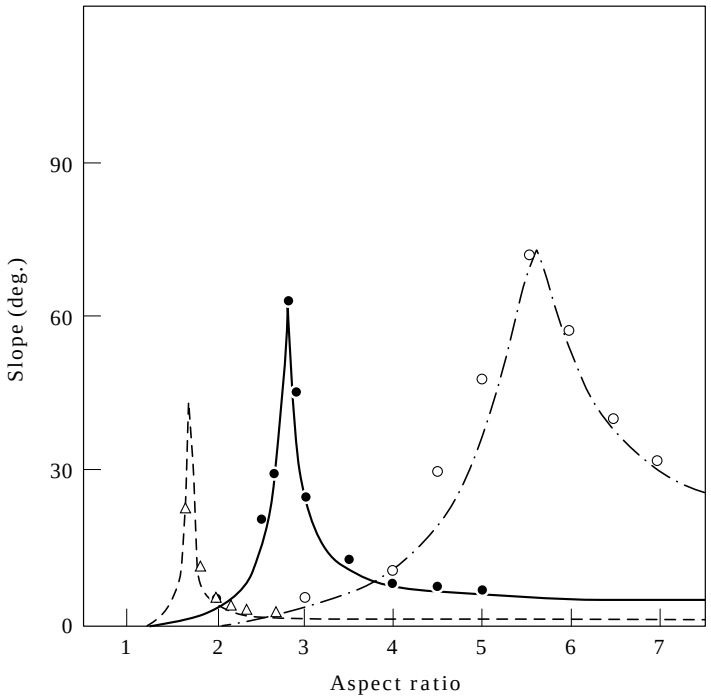

Figure 9. Slope variation of the second flexural mode (symmetric laminates). Ritz: –·–·–, $\theta = 15°$; – – –, $\theta = 30°$; ——, $\theta = 45°$. Experimental: ○, $\theta = 15°$; ●, $\theta = 30°$; △, $\theta = 45°$.

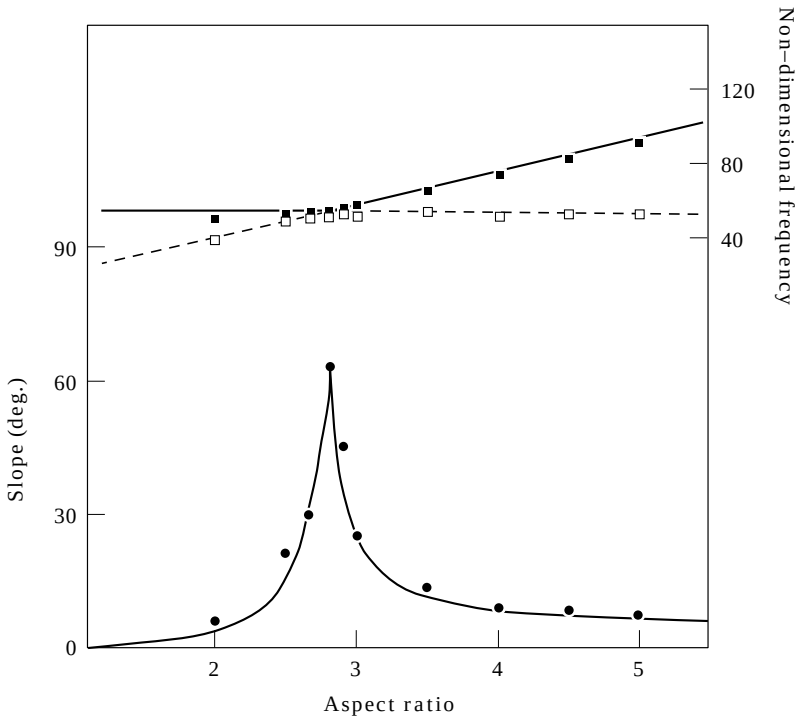

Figure 10. Comparison of slope variation of the second flexural mode and non-dimensional frequencies ($\theta = 30°$, symmetric laminate). Top: Ritz; ——, 2nd mode; – – –, 3rd mode. Experimental: □, 2nd mode; ■, 3rd mode. Bottom: ——, Ritz; ●, experimental.

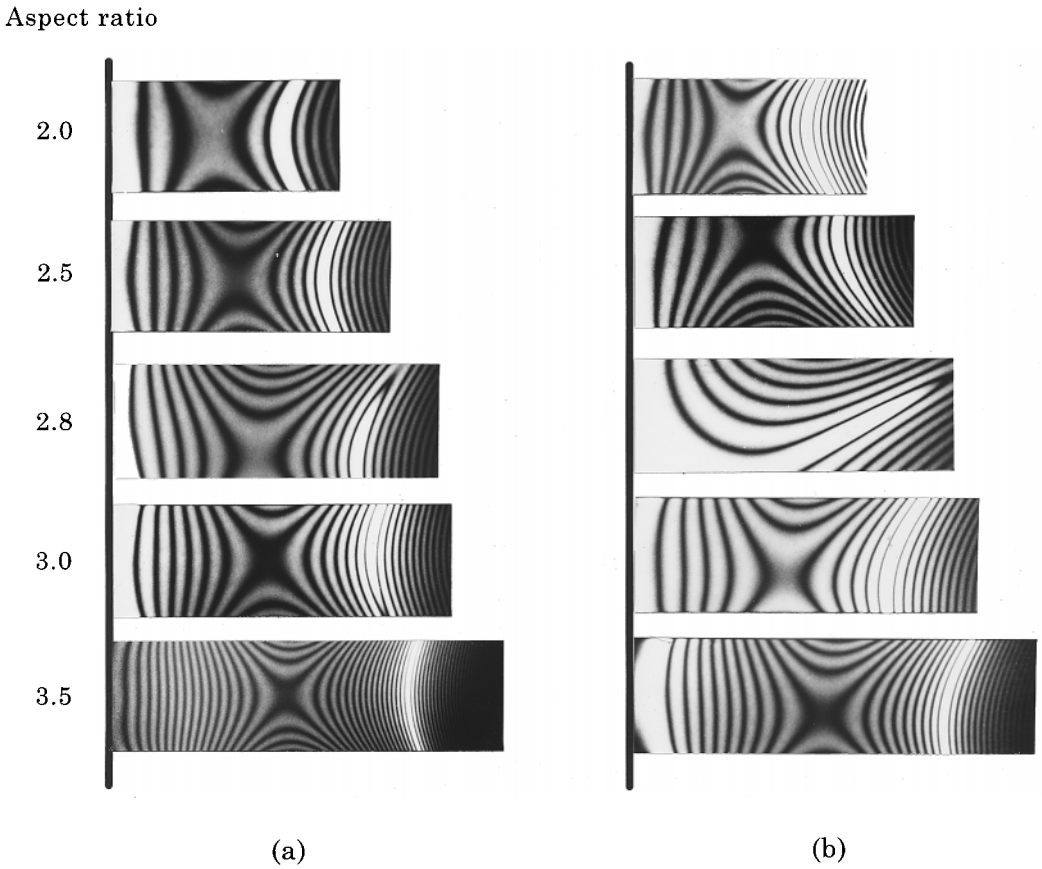

Figure 11. Comparison of slope variation ($\theta = 30^\circ$ laminates). (a) Anti-symmetric; (b) symmetric.

by the Ritz method and the experimentally measured values can be seen in Figure 9. Therefore, it can be theoretically predicted that the coupling effect still remains when the aspect ratio is increased enough, and takes a constant value in the limit corresponding to the case of a beam. Since these minimum slopes are expected to be different for different fiber orientations, as noted in Figure 9, the effect of coupling with respect to fiber orientation could also be established.

The above mentioned coupling behavior of symmetric laminates close to the degeneration point thus implies further examination is required into the effect of resonance frequencies of these types of laminates close to the degeneration point. For this purpose, the slope variation of a 30° symmetric laminate was considered next by comparing it with the variations of the resonance frequencies as shown in Figure 10, in which the peak of the slope variation is found to be near the point where the resonance frequencies of the second and third modes are almost the same. In general, such a point where two frequencies are exactly identical is called a degeneration point. At this point, a flexural–torsional coupling behavior can be observed even for the special anti-symmetric laminates, and incidentally for isotropic plates also. However, from the comparison of the fringe patterns presented in Figure 11, it is evident that the change of the vibrational mode shape is caused by the presence of the coupling stiffness. This is due to the fact that the mode shapes for the special anti-symmetric laminate in Figure 11(a) are symmetrical for

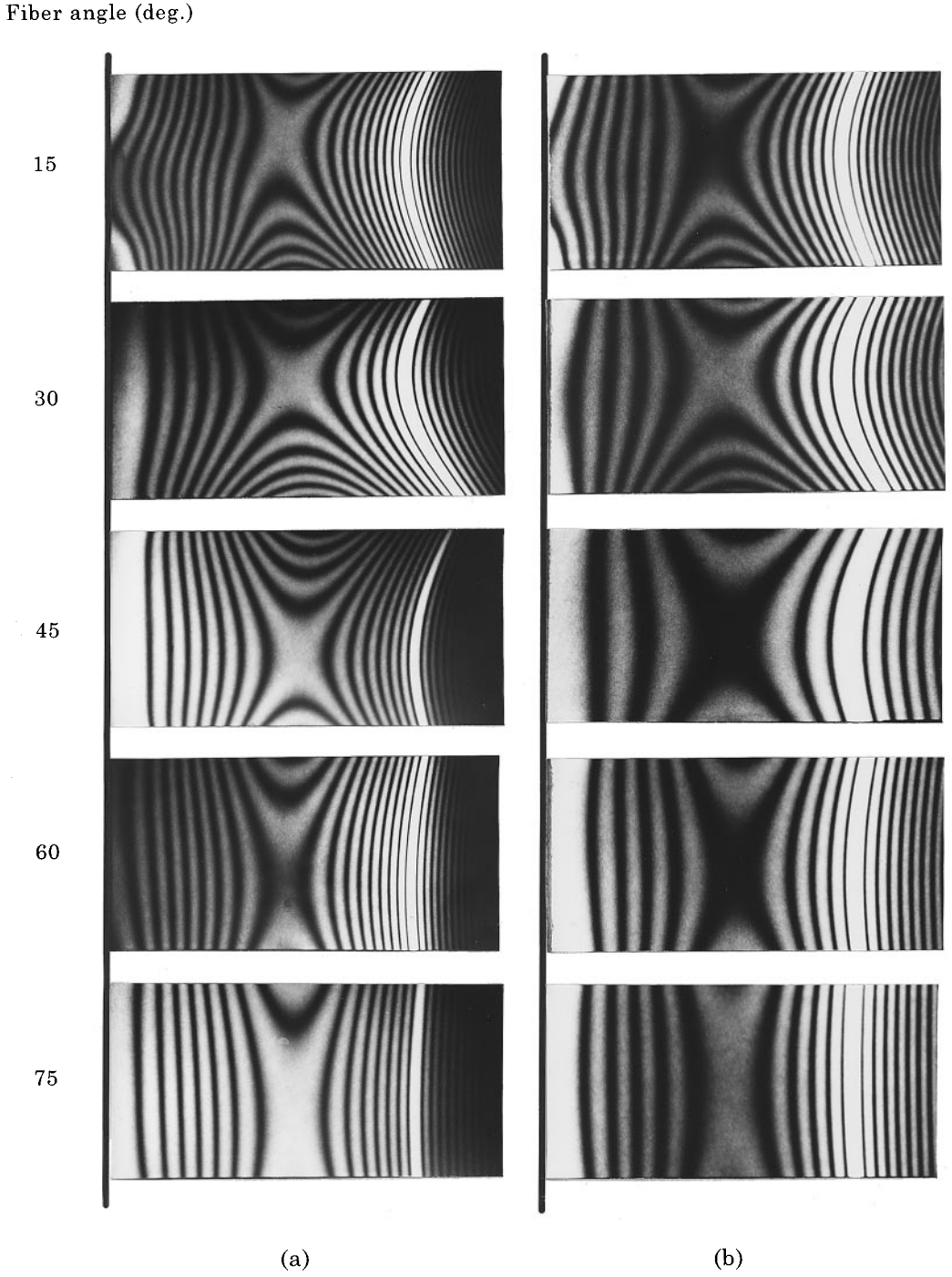

Figure 12. Fringe patterns of the second flexural mode (symmetric laminates). (a) 120 × 60 mm; (b) 60 × 30 mm.

all the cases except for the case of one aspect ratio, namely 2·8, whereas the fringe patterns of the symmetric laminate in Figure 11(b) are unsymmetrical over a wide range of the aspect ratio.

Additionally, the fringe patterns of the second flexural mode are shown in Figure 12 for the symmetric laminates which have the same aspect ratio but different dimensions measuring 120×60 mm and 60×30 mm, respectively. For each fiber orientation, the fringe patterns between these two types of laminates are found to be almost identical to each other. Therefore, it is understood that the plate aspect ratio becomes an important variable in determining the vibrational mode shape of cantilevered plate, and it can also be considered that the degree of the flexural–torsional coupling effect on the vibrational mode shape is identical for plates having the same aspect ratios.

5. CONCLUSIONS

Laser holographic interferometry has been applied to investigate the effect of flexural–torsional coupling stiffness on the vibrational characteristics of angle-ply laminates. It has been verified both experimentally and analytically that the coupling effect on the resonance frequencies is very marginal in the case of the symmetric laminated plate model studied here. However, the vibrational mode shapes are significantly affected by the flexural–torsional coupling stiffness. Again, it is found that the degree of this coupling effect of symmetric laminates depends both on the fiber orientation and the aspect ratio of the test specimen. Moreover, it should be noted that the coupling effect on the vibrational mode shape becomes maximum at the point where the resonance frequencies of different modes are closely spaced. In the neighborhood of this degeneration point, laminates having no coupling stiffness, namely orthotropic and even isotropic plates, will also show flexural–torsional coupling behaviors. Finally, although the resonance frequencies are generally overestimated by the Ritz method, it is found that the vibrational mode shapes can be predicted with reasonably good accuracy by such a simple method.

REFERENCES

1. E. F. Crawley and J. Dugundji 1980 *Journal of Sound and Vibration* **72**, 1–10. Frequency determination and non-dimensionalization for composite cantilever plates.
2. Y. Narita and A. W. Leissa 1992 *Journal of Sound and Vibration* **154**, 161–172. Frequencies and mode shapes of cantilevered laminated composite plates.
3. H. Fukunaga, H. Sekine and M. Sato 1994 *Journal of Sound and Vibration* **171**, 219–229. Optimal design of symmetric laminated plates for fundamental frequency.
4. D. W. Jensen and E. F. Crawley 1984 *AIAA Journal* **22**, 415–420. Frequency determination techniques for cantilevered plates with bending–torsion coupling.
5. P. A. A. Laura and E. Romanelli 1974 *Journal of Sound and Vibration* **37**, 367–377. Vibrations of rectangular plates elastically restrained against rotation along all edges and subjected to a bi-axial state of stress.
6. P. A. A. Laura and R. Duran 1975 *Journal of Sound and Vibration* **42**, 129–135. A note on forced vibrations of a clamped rectangular plate.
7. M. S. Qatu 1991 *International Journal of Solids Structures* **28**, 941–954. Free vibration of laminated composite rectangular plates.
8. H. Fukunaga, H. Sekine and H. Tsutsui 1995 *Journal of the Japan Society of Mechanical Engineers* **61**, 4168–4174. Effects of laminate configurations and bending–torsional coupling on vibrational characteristics of cantilevered laminated plates (in Japanese).
9. R. R. Clary 1972 in *Composite Materials*: *Testing and Design*, *ASTM STP* **497**, 415–438. American Society for Testing and Materials. Vibration characteristics of unidirectional filamentary composite material panels.

10. G. Caprino and I. C. Visconti 1982 *Journal of Composite Materials* **16**, 395–399. A note on specially orthotropic laminates.
11. *ASTM* D3039-76 1989 American Society for Testing of Materials. Standard test method for tensile properties of fiber-resin composites.
12. *ASTM* D3518-76 1982 American Society for Testing of Materials. Standard practice for inplane shear stress–strain response of unidirectional reinforced plastics.